How plasma parameters fluctuations influence emissive probe measurements

G. Bousselin, N. Plihon, N. Lemoine, J. Cavalier, and S. Heuraux

Citation: Physics of Plasmas **22**, 053511 (2015); doi: 10.1063/1.4921643
View online: http://dx.doi.org/10.1063/1.4921643
View Table of Contents: http://scitation.aip.org/content/aip/journal/pop/22/5?ver=pdfcov
Published by the AIP Publishing

PHYSICS OF PLASMAS 22, 053511 (2015)

How plasma parameters fluctuations influence emissive probe measurements

G. Bousselin,[1,a)] N. Plihon,[1] N. Lemoine,[2] J. Cavalier,[3] and S. Heuraux[2]
[1]*Laboratoire de Physique, École Normale Supérieure de Lyon, CNRS & Université de Lyon, 46 allée d'Italie, 69364 Lyon Cedex 07, France*
[2]*Institut Jean Lamour IJL, Université de Lorraine, UMR 7198 CNRS, Vandoeuvre-les-Nancy, France*
[3]*Institute of Plasma Physics ASCR v. v. i., Prague, Czech Republic*

(Received 25 February 2015; accepted 6 May 2015; published online 26 May 2015)

Relationship between the floating potential of an emissive probe and plasma potential oscillations is studied in the case of controlled oscillations of plasma parameters. This relationship is compared to a quasi-static model for floating potential oscillations that assumes a constant emission current and includes the fluctuations of plasma parameters (density and electron temperature). Two different plasma regimes are considered. In the first one, the model is coherent with experimental results. In the second, the model does not fulfill one of the assumption due to the evidence of emission current oscillations when the mean emission current exceeds a given threshold. This second regime highlights the importance of taking into account emission current oscillations in the interpretation of emissive probe measurements. Nevertheless, discrepancies are still observed between emissive probe floating potential and plasma potential oscillations. © *2015 AIP Publishing LLC.*
[http://dx.doi.org/10.1063/1.4921643]

I. INTRODUCTION

A quantitative evaluation of turbulent transport in plasmas requires reliable measurements of electric fields and plasma parameters fluctuations in amplitude and phase. Among the variety of electrostatic probes, electron emissive probes[1] are widely used both in laboratory[2,3] and in fusion devices[4–8] plasmas to directly measure the plasma potential fluctuations and then estimate electric fields fluctuations. These probes usually consist of a refractory metal electrode directly or indirectly heated (using an external electrical power supply or high intensity lasers). For a sufficiently high electrode temperature, the probe emits electrons when negatively biased with respect to the plasma potential. In a conventional Maxwellian plasma, the relationship between the emissive probe floating potential $\phi_{fl,em}$ and the plasma potential ϕ_p (expressed in Volts) is given by

$$\phi_{fl,em} = \phi_p - T_e \ln\left(\frac{I_{es}}{I_{is} + I_{em}}\right), \tag{1}$$

where T_e is the electron temperature expressed in eV, I_{es} and I_{is} are the absolute values of the electron and ion saturation currents, respectively, and I_{em} is the emission current.

Using this model, the emissive probe floating potential $\phi_{fl,em}$ tends towards the plasma potential ϕ_p when the emission current is adjusted to the level of the electron saturation current (i.e., $I_{es} = I_{is} + I_{em} \approx I_{em}$ because $I_{es} \gg I_{is}$ in the previous relation). It is then usually accepted that the measurement of the floating potential of the emissive probe provides a direct measurement of the plasma potential. While this is probably true to measure the time-averaged plasma potential, as shown by many successful measurements performed in laboratory[9–11] and fusion devices[5] plasmas worldwide, the question whether it is possible to directly and reliably estimate the plasma potential fluctuations using the floating potential fluctuations of an emissive probe remains open. This statement can be understood if one recall that I_{es} and I_{is} oscillate as the product of the electron density times the square root of the electron temperature ($n\sqrt{T_e}$) and that I_{em} does not follow necessary these oscillations. In a recent paper,[12] a modeling of floating potential fluctuations of an emissive probe has been proposed. In the frame of this model, plasma parameters are assumed to oscillate slowly compared to the inverse of ion plasma frequency, so that the sheath around the probe can be considered at equilibrium at any time so that Eq. (1) still holds. Floating potential fluctuations are approximated by the first order term of $\phi_{fl,em}$ in Eq. (1), obtained by differentiating Eq. (1) considering that both saturation currents are proportional to the plasma density and the square root of the electron temperature and assuming a constant emission current independent of the plasma parameters. Potential effects of space-charged limitation[13,14] and secondary emission on the emission current have been neglected. Then emissive probe floating potential fluctuations read

$$\tilde{\phi}_{fl,em} = \tilde{\phi}_p - \langle T_e \rangle \left(\frac{\langle I_{em} \rangle}{\langle I_{is} + I_{em} \rangle}\right) \frac{\tilde{n}}{\langle n \rangle} - \left[\ln\left(\frac{\langle I_{es} \rangle}{\langle I_{is} + I_{em} \rangle}\right) + \frac{1}{2}\left(\frac{\langle I_{em} \rangle}{\langle I_{is} + I_{em} \rangle}\right)\right] \tilde{T}_e, \tag{2}$$

with the following notation: $f = \langle f \rangle + \tilde{f}$, where $\langle f \rangle$ stands for time-averaging of the parameter f and $\tilde{f}$ stands for the fluctuating part of f.

In the frame of this first order model, $\langle \phi_{fl,em} \rangle$ tends towards $\langle \phi_p \rangle$ when the emission current $\langle I_{em} \rangle$ reaches the average of the electron saturation current $\langle I_{es} \rangle$ (in the remainder

a)guillaume.bousselin@ens-lyon.fr

of this article, we will denote this specific value I_{em}^*)—note that this situation is sometimes referred to as "emissive probe floating at the mean plasma potential." However, the above simple model highlights that the floating potential fluctuations $\tilde{\phi}_{fl,em}$ of an emissive probe depend not only on the plasma potential fluctuations $\tilde{\phi}_p$ but also on electron density and electron temperature fluctuations. Equation (2) has been experimentally validated on the laboratory plasma device Mirabelle[10,12] assuming negligible electron temperature fluctuations and a Boltzmann relation between plasma density and plasma potential fluctuations.

We report in this article an improved experimental validation of this model in instability-free regimes where the plasma excitation is externally sinusoidally modulated. This validation is based on a time-resolved current-voltage characteristics reconstruction method allowing to measure the synchronized time series of $\tilde{\phi}_p$, $\tilde{n}$ and $\tilde{T}_e$, without considering any hypothesis concerning the amplitude of the different plasma parameters fluctuations nor phase relations between them.

The article is organized as follows. The experimental setup and measurements methods in presence of external modulation are described in Sec. II. The fluctuations of plasma parameters and of emissive probe floating potential are analyzed in detail in Sec. III in the case of two different regimes. The importance of emission current oscillations is discussed in Sec. IV. Conclusions relative to the validity of this model and of the estimate of plasma potential oscillations given by floating potential measurement of an emissive probe are given in Sec. V.

II. EXPERIMENTAL SETUP AND METHODS

A. Experimental setup

Experiments have been carried out on the von-Kármán plasma experiment (VKP), sketched in Fig. 1 and described in details in Ref. 15. It consists of a cylindrical magnetized plasma device in which the plasma production is achieved by a 13.56 MHz radio-frequency (RF) power generator (up to 1.4 kW) coupled to a 3-turn antenna through a L-type matching network. Bitter coils are used to produce an axial magnetic field (2–200 mT) that confines the plasma in the cylindrical section (700 mm length and 200 mm diameter). Argon gas is used to generate the plasma at an usual working pressure range of 0.1–10 mTorr. In these conditions, the electron density range is between 10^{16} and $10^{18}\,\mathrm{m}^{-3}$ and the electron temperature range is typically 2–6 eV.

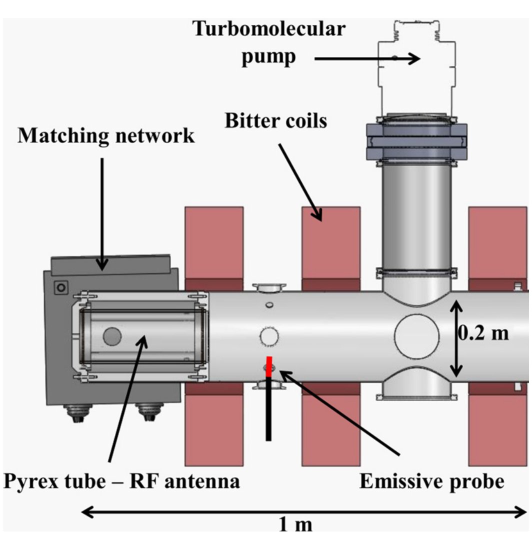

FIG. 1. Scheme of the von-Kármán plasma experiment (VKP).

Measurements have been performed using a conventional emissive probe consisting of a tungsten wire loop (8 mm length and 0.2 mm diameter) heated by a DC current I_h provided by an external floating power supply. Due to the complexity to integrate a RF compensation system to emissive probe, all the measurements presented in this article have been done using a non-compensated probe. Nevertheless, a comparison between current-voltage characteristics recorded using conventional Langmuir probe and RF compensated[16] Langmuir probe has been previously performed in VKP. No significant differences between the values of the plasma potential and the saturation currents obtained with the two different probes have been observed while the electron temperature difference was less than 5%. This validates the use of the non-compensated emissive probe.

Signals have been acquired using a National Instruments PXI SMU 4132 for the control of the biasing voltage of the probe and PXI 4472 acquisitions cards for the current and voltage measurements, with a 24-bits resolution.

B. Oscillation measurements using reconstruction method

In order to test the validity of the model described by Eq. (2), a precise estimation of all the fluctuating quantities ($\tilde{\phi}_{fl,em}$, $\tilde{\phi}_p$, $\tilde{n}$, and $\tilde{T}_e$) in amplitude and phase is needed. Obtaining such measurements is complex when fluctuations are driven by plasma instabilities. To facilitate these measurements, experiments have been performed in plasma regimes wherein the RF power transferred to the plasma has been modulated using an external sinusoidal generator (in regimes where the plasma is instability-free). This periodic power modulation, at a period $T = 1$ ms much longer than the radio-frequency period, allows to generate artificial but stationary and non drifting plasma fluctuations. The modulation frequency has been chosen to set in the typical range of low-frequency plasma instabilities. These periodic plasma parameters modulations can be reliably measured using a method of time-resolved current-voltage characteristics reconstruction of the cold (Langmuir) probe, as presented in reference.[17] This method can be described as follows: the cold probe (i.e., without heating current flowing through the probe wire loop) is biased at a fixed potential and measures the current collected during a time $t = 100T$ at a sampling frequency $f_s = 50/T = 50$ kHz. The modulation signal is recorded simultaneously and is used as a phase reference. Once both signals have been recorded, the process is iterated by changing the probe bias potential. Scanning large interval of bias potential from negative to positive values with respect to ϕ_p, by steps sufficiently small to obtain a good resolution, it is then possible to reconstruct a current-voltage (I-V) characteristic at each time of the modulation signal. These time resolved *I-V* curves are then processed and allow to obtain synchronized time series for the different plasma parameters. These times series thus allow to reconstruct the plasma density $\tilde{n}$, the plasma potential $\tilde{\phi}_p$ and the electron temperature $\tilde{T}_e$ oscillations over one period T, by averaging over 100 periods. Both time-averaged values and oscillations (phase and amplitude) of plasma parameters can then be extracted with this method.

The instantaneous time series of the floating potential of emissive probe $\tilde{\phi}_{fl,em}(t)$ for increasing value of the heating current is measured according to the procedure proposed in Ref. 12. During the plasma modulation, the emissive probe is progressively heated by increasing the DC heating current I_h, from $I_h = 0$ A (cold probe) to around 7 A (an intensity sufficiently important for the emissive probe to float at the mean plasma potential, as demonstrated in Subsection III A). For each heating current intensity, a time series ($t = 100T$) of the emissive probe floating potential $\phi_{fl,em}(t)$ is recorded simultaneously with the modulation signal. These time series are then filtered using a lowpass digital Butterworth filter at a cutoff frequency $f_c = 5$ kHz to remove the high-frequency noise while keeping informations around the frequency modulation $1/T = 1$ kHz.

C. Plasma and emissive probe mean parameters

Mean plasma parameters are estimated from the reconstructed time series of the cold probe yielding $\langle T_e\rangle$, $\langle I_{es}\rangle$, $\langle I_{is}\rangle$, $\langle \phi_p\rangle$, and $\langle n\rangle$.

Mean *I-V* emissive probe characteristics are obtained for increasing values of the DC heating current I_h (then for increasing values of the emission current I_{em}) using a potential ramp whose period is much larger than the RF modulation period. Fig. 2 shows typical examples of time-averaged current-voltage characteristics of the emissive probe for various values of I_h. The classical symmetrization of the *I-V* curves when increasing the heating current is observed. The emission current I_{em} is extracted from these current-voltage characteristics, following Ref. 12. Let us denote $\langle \phi_{fl,em}(I_h)\rangle$ the time-averaged floating potential of the emissive probe

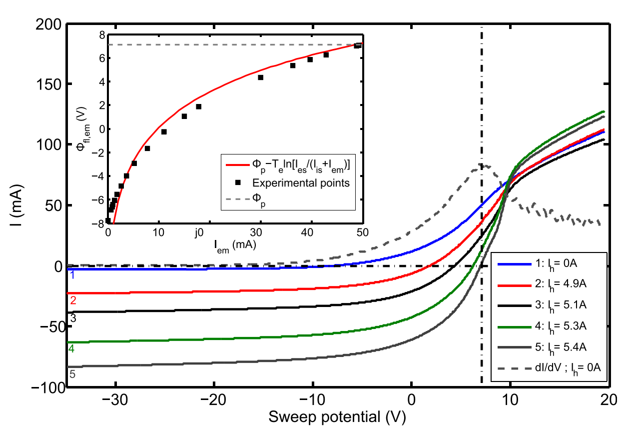

FIG. 2. *I-V* characteristics of the emissive probe for several heating current values I_h. Inset: Experimental and theoretical (Eq. (1)) evolution of the emissive probe mean floating potential $\langle \phi_{fl,em}\rangle$ as a function of the emission current I_{em}.

heated at I_h. For a given value of I_h, the emission current $I_{em}(I_h)$ is then defined as the value of the cold probe characteristic current at $\langle \phi_{fl,em}(I_h)\rangle$.[18] It is then possible to plot the emissive probe parameters ($\langle \phi_{fl,em}\rangle$, $\langle \tilde{\phi}^2_{fl,em}\rangle$) as a function of I_{em} instead of I_h.

D. Testing model validity

The purpose of this paper is to quantify the influence of low-frequency oscillations (seen as controlled fluctuations) $\tilde{n}$ and $\tilde{T}_e$ on the relationship between $\tilde{\phi}_{fl,em}$ and $\tilde{\phi}_p$. The methods presented in Subsections II B and II C make it possible to compare emissive probe floating potential and plasma potential in phase and amplitude and to test the validity of the quasi-static model assuming constant emission current. Therefore, the experimental standard deviation of emissive probe floating potential $\sigma_{\tilde{\phi}_{fl,em}}$ is compared to its theoretical expression obtained from Eq. (2)

$$\begin{aligned}\langle \tilde{\phi}^2_{fl,em}\rangle = \langle \tilde{\phi}^2_p\rangle + \langle T_e\rangle^2 C_1^2 \frac{\langle \tilde{n}^2\rangle}{\langle n\rangle^2} \\ -2\langle T_e\rangle C_1 \frac{\langle \tilde{\phi}_p \tilde{n}\rangle}{\langle n\rangle} + C_2^2 \langle \tilde{T}_e^2\rangle \\ -2C_2\langle \tilde{T}_e \tilde{\phi}_p\rangle + 2\langle T_e\rangle C_1 C_2 \frac{\langle \tilde{T}_e \tilde{n}\rangle}{\langle n\rangle},\end{aligned} \tag{3}$$

$$\sigma_{\tilde{\phi}_{fl,em}} = \langle \tilde{\phi}^2_{fl,em}\rangle^{1/2}, \tag{4}$$

with $C_1 = \frac{\langle I_{em}\rangle}{\langle I_{is}+I_{em}\rangle}$, $C_2 = \ln\left(\frac{\langle I_{es}\rangle}{\langle I_{is}+I_{em}\rangle}\right) + \frac{1}{2}C_1$.

To calculate the theoretical value of Eq. (3), the fluctuating times series $\tilde{\phi}_p$, $\tilde{n}$, and $\tilde{T}_e$ as well as the mean value $\langle n\rangle$, $\langle T_e\rangle$, $\langle I_{es}\rangle$, and $\langle I_{is}\rangle$ can be estimated from the reconstructed time series of the cold probe. All parameters of this model are measured experimentally so that there are no adjustable parameters.

Since all the plasma fluctuations ($\tilde{\phi}_p$, $\tilde{T}_e$, and $\tilde{I}_{es} \propto \tilde{I}_{is} \propto n\widetilde{\sqrt{T_e}}$) can be precisely estimated (thanks to the experimental procedure of external plasma modulation), a second calculation of the theoretical values $\sigma_{\tilde{\phi}_{fl,em}}$ can be performed using the full model without differentiation described by Eq. (1).

The main interest of the first order model is to clearly explicit the dependence of the emissive probe floating potential fluctuations with the plasma potential, the plasma density, and the electron temperature fluctuations. It allows indeed a better understanding of the role of both the amplitude of the different plasma parameter fluctuations and the phase relation between them.

The goal of this article is to experimentally validate the model of Eqs. (2) and (3). In order to achieve this goal, we have driven stationary plasma fluctuations by modulating the radio-frequency power injected to the plasma. The resulting plasma parameters oscillations are characterized by different phase shifts between the various plasma parameters; and allow to validate the effect of these phase shifts on the evolution of the floating potential of emissive probe as function of the emission current as predicted by Eqs. (2) and (3). At leading order, the amplitude of the plasma parameters modulation is set by the amplitude of the power modulation and can be easily controlled. We restricted ourselves to low amplitude (between 1% and 2%) of plasma parameters fluctuations such that the first order description remains valid. A precise control of the phase shifts between the different plasma parameters modulations is more complex. A detailed modeling of the plasma parameters modulation requires detailed particle and power balance equations[19] and a model for power deposition from the radio-frequency electromagnetic field to the electrons and losses to the walls. This task is extremely complex and beyond the scope of the present article (we recall that we focus on the validity check of the use of emissive probes). In our setup, ionization in volume is the dominant source of charged particles and losses to the vessel walls is the dominant loss process, and the energy is entirely coupled to the electrons. Global particle and power balances thus read

$$\frac{dn}{dt}(t) = S_i(t) - \frac{A}{V}\Gamma_{wall}(t), \tag{5}$$

$$\frac{d}{dt}\left(\frac{3}{2}n(t)k_B T_e(t)\right) = P_{abs}(t) - P_{loss}(t), \tag{6}$$

where $S_i(t)$ is the instantaneous volume ionization (the particle source term); $\Gamma_{wall}(t)$ is the ion outflow at the walls; A and V are the surface of the vessel chamber and the discharge volume, respectively; and P_{abs} and P_{loss} correspond to the power absorbed and the power lost by the electrons, respectively. A precise understanding of the plasma parameters modulation would require a detailed modeling of the right hand side terms of the above equations, while the injected power is sinusoidally modulated. For a fixed geometry, volume ionization walls losses depend on the working gas pressure and the magnetic field. Determining P_{abs} is a complex problem that requires a precise model of the energy deposition from the r.f. electromagnetic fields to the electrons (depending on the electromagnetic field distribution and electrons heating processes). Electrons can dissipate the energy trough collisions with the gas (elastic or inelastic collisions) or by carrying kinetic energy to the boundaries. All these processes strongly depend on the gas pressure and the magnetic field. A precisely estimate of all these loss mechanisms is a difficult task which is out of the scope of this paper. However, we can clearly understand that modifications of the discharge parameters such as the working pressure or the magnetic field allow to change the phase shifts between plasma parameters modulation.

Several experiments have been conducted in regimes characterized by different pressure, r.f. injected power and magnetic fields. In this article, we chose to focus on two specific regimes. These two regimes have been selected for different evolutions of $\sigma_{\tilde{\phi}_{fl,em}}$ with I_{em} as precisely described Sec. III: in regime 1, $\sigma_{\tilde{\phi}_{fl,em}}$ increases with I_{em}, while it decreases in regime 2. The interesting point is that similar evolutions of $\sigma_{\tilde{\phi}_{fl,em}}$ with I_{em} have been observed both in laboratory plasmas[20] and tokamak plasmas[4] in the presence of natural instabilities. The direct comparison between our two regimes and the instabilities observed in Refs. 20 and 4 should be taken with care since in our setup we drive non drifting controlled modulations, while the above mentioned references deal with natural instabilities. However, while the evolutions in the presence of natural instabilities have been explained by the influence of electrons temperature fluctuations only, our investigation show that other processes could also explain similar trends. We indeed show in the following that these trends should be explained by considering the amplitude and phase of all the plasma parameters fluctuations as described by Eqs. (2) and (3).

III. EXPERIMENTAL RESULTS

The model is tested in the case of two different plasma regimes. The first plasma regime is characterized by an argon working pressure of 3 mTorr and an axial magnetic field of 6 mT. In this regime, the RF power has been modulated with a 5% relative amplitude around 280 W (±14 W). In the second regime, the argon working pressure and the magnetic field intensity were reduced to 1 mTorr and 3 mT, respectively. The RF power has also been modulated with a 5% relative amplitude around 420 W (±21 W).

A. Mean plasma parameters and evolution of time-averaged emissive probe floating potential with I_{em}

The mean plasma parameters as measured from a *I-V* characteristic recorded when the probe is cold are given in Table I. For the first regime, we find $\langle \phi_p \rangle = 7.1$ V, $\langle T_e \rangle = 4.6$ eV, and $\langle n \rangle = 1.4 \times 10^{17}\,\mathrm{m}^{-3}$. In the second regime, the mean plasma parameters are $\langle \phi_p \rangle = 12.5$ V, $\langle T_e \rangle = 5.6$ eV, and $\langle n \rangle = 9.2 \times 10^{16}\,\mathrm{m}^{-3}$. Mean electron density estimates are rough as it is difficult to estimate properly the actual collecting surface of the tungsten loop, but the ratio of the two densities should be correct.

In both regimes, it has been checked that $\langle \phi_{fl,em} \rangle$ tends towards $\langle \phi_p \rangle$ when increasing I_{em}. In this subsection, one will only focus on the first regime, the results obtained in the second regime being very similar.

The evolution of the time averaged emissive probe floating potential $\langle \phi_{fl,em}(I_{em}) \rangle$ as a function of the emission current I_{em} is displayed in the inset of Fig. 2. At $I^*_{em} = I_{es} = 50$ mA (corresponding to a heating current $I_h = 5.4$ A), the emissive probe floats at the mean plasma potential

TABLE I. Discharge and mean plasma parameters for the two studied regimes.

	Regime 1	Regime 2
Argon pressure (mTorr)	3	1
B field (mT)	6	3
RF mean power (W)	280	420
RF modulation (%)	5	5
$\langle T_e \rangle$ (eV)	4.6	5.6
$\langle \phi_p \rangle (V)$	7.1	12.5
$\langle I_{es} \rangle$ (mA)	50	35
$\langle I_{is} \rangle$ (mA)	0.8	0.6
$\langle n \rangle$ (m^{-3})	1.2×10^{17}	9.2×10^{16}

(determined from the maximum derivative of the cold probe characteristic): $\langle \phi_{fl,em}(I^*_{em}) \rangle = \langle \phi_p \rangle$.

Using the time-averaged plasma parameters measured from the cold probe characteristics, the theoretical evolution of $\langle \phi_{fl,em}(I_{em}) \rangle$ using Eq. (1) is also displayed as a full (red) line. Note that there are no fitting parameters in this computation using the parameter values for regime 1 in Table I obtained after processing the cold emissive probe characteristic. The good agreement between the experimental points and the theoretical ones calculated without any fitting parameters demonstrates that Eq. (1) is valid when considering time averaged quantities.

We can now focus on the dependence of the emissive probe floating potential fluctuations with the plasma parameters fluctuations.

B. Influence of plasma parameter oscillations and of their relative phases on amplitude and phase of emissive probe floating potential fluctuations

In this subsection, we study the relationship between the amplitude of plasma potential and emissive probe floating potential fluctuations for different emission currents, compare it with the relationship expected from the quasi-static model. We also investigate the relative phase between plasma potential and emissive probe floating potential fluctuations for the first regime and then for the second regime.

The plasma potential time series $\phi_p(t)$ is obtained from the reconstruction method of the cold probe as described above. The experimental value of the standard deviation of emissive probe floating potential fluctuations $\sigma_{\tilde{\phi}_{fl,em}}$ is calculated using the time series $\phi_{fl,em}(t)$.

The evolution of $\sigma_{\tilde{\phi}_{fl,em}}$ as a function of the emission current (black squares) in the first regime is displayed in Fig. 3. When increasing I_{em}, $\sigma_{\tilde{\phi}_{fl,em}}$ decreases and reaches a value slightly lower than the standard deviation of $\tilde{\phi}_p$ (grey line) when $I_{em} = I^*_{em} = 50\,\mathrm{mA}$ (i.e., when the time-averaged floating potential of the emissive probe equals the time-averaged plasma potential as demonstrated in Subsection III A). The first observation is that the oscillation amplitude of both potentials when $I_{em} = I^*_{em}$ are quite close (the amplitude of $\tilde{\phi}_{fl,em}(t)$ is 15% smaller than the one of $\tilde{\phi}_p(t)$).

Let us now compare the first order model to the experimental evolution of the emissive probe floating potential fluctuations with I_{em}.

The theoretical value of $\sigma_{\tilde{\phi}_{fl,em}}$ calculated using Eq. (3) is displayed in Fig. 3 as a (red) full line. The first order model reflects quite well the experimental trend especially taking into account that it has been calculated without any fitting parameters. In addition, the model being quite sensitive to the amplitude and phase of the different plasma parameters, these results also attest the reliability of the time-resolved *I-V* curves reconstruction method that has been used. Then, the hypothesis of a constant emission current is not incoherent with experimental results from the first regime, even if the model predicts that $\sigma_{\tilde{\phi}_{fl,em}}$ should be a bit larger than the standard deviation of the plasma potential, whereas the experimental value is close to it and even slightly smaller.

A second calculation of the theoretical values $\sigma_{\tilde{\phi}_{fl,em}}$ has been performed using the full model without differentiation described by Eq. (1). The results (blue dashed line) are depicted in Fig. 3 as a function of the emission current. The first order model is an excellent approximation of the full relation. In this regime, the level of fluctuations is relatively small (≈2% see Fig. 4(a)). Consequently, there is no need to go to higher differentiation order to better represent the experimental evolution of $\sigma_{\tilde{\phi}_{fl,em}}$.

A further analysis is obtained by comparing time series of $\tilde{\phi}_{fl,em}(t)$ and $\tilde{\phi}_p(t)$. Fig. 4(a) shows the time series of the plasma parameters relative modulation $\tilde{n}$, $\tilde{T}_e$, and $\tilde{\phi}_p$ obtained from the cold probe reconstruction method, together with the time series of $\tilde{\phi}_{fl,em}(t)$ for $I_{em} = I^*_{em}$. A non-negligible phase-shift around 35° between $\tilde{\phi}_{fl,em}(t|I_{em} = I^*_{em})$ and $\tilde{\phi}_p(t)$ is measured.

Let us now investigate the results from the second plasma regime described in Subsection III A. The relative amplitude of the reconstructed fluctuations $\tilde{\phi}_p$, $\tilde{n}$, and $\tilde{T}_e$ are

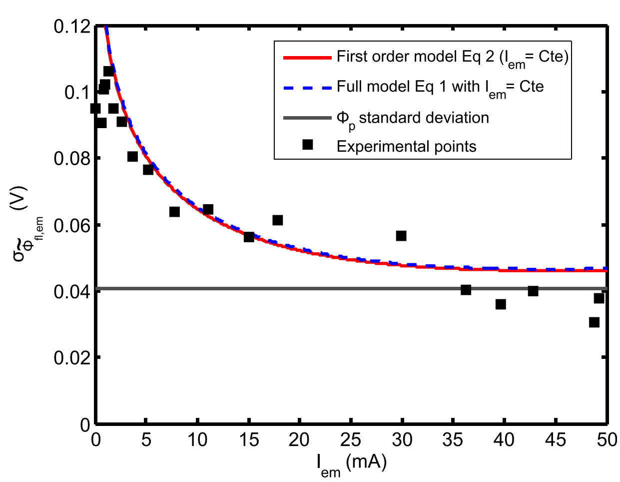

FIG. 3. Standard deviation of the emissive probe floating potential fluctuations $\sigma_{\tilde{\phi}_{fl,em}}$ as a function of the emission current in the regime 1; squares: experimental values, full line: theoretical values calculated using the first order model (Eqs. (2) and (3)), dashed line: theoretical values calculated using the full model (Eq. (1)).

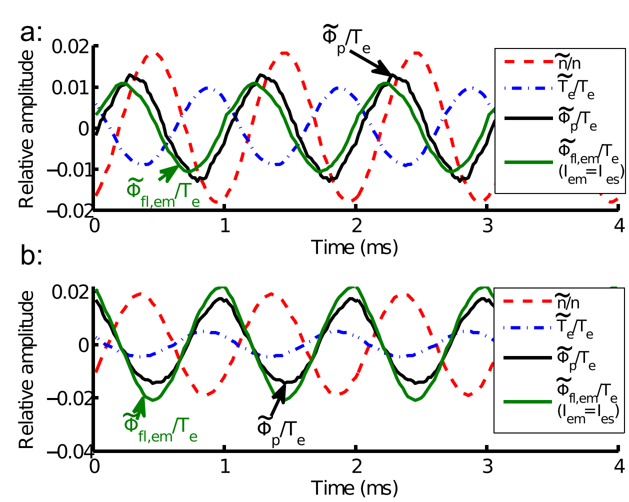

FIG. 4. Time series of the relative amplitude of the plasma fluctuations ($\tilde{\phi}_p$, $\tilde{n}$, and $\tilde{T}_e$) in (a) regime 1; (b) regime 2. The time series of the emissive probe floating potential fluctuations corresponding to $I_{em} = I^*_{em} = I_{es}$ are superimposed to the plasma fluctuations.

TABLE II. Phase shift between the different plasma fluctuations in the two plasma regimes.

	Phase shift $\tilde{\phi}_p$; $\tilde{n}$	Phase shift $\tilde{\phi}_p$; $\tilde{T}_e$
Regime 1	$+65°$	$-144°$
Regime 2	$+137°$	$-50°$

depicted in Fig. 4(b). These amplitudes are similar to those observed in the first regime; however, their phase relations are clearly different (see Table II). According to Eqs. (2) and (3), a change of phase relation between the fluctuating plasma quantities should modify the evolution of the emissive probe floating potential fluctuations when increasing the emission current. This evolution, experimentally measured using the same procedure as the one used for the first regime, is shown in Fig. 5 as a function of the emission current (black squares) and strongly differs from the one observed in the first regime. The standard deviation increases when I_{em} increases from 0 to 15 mA, overpassing the standard deviation of $\tilde{\phi}_p(t)$. For I_{em} values above 15 mA, a discontinuity is observed and $\sigma_{\tilde{\phi}_{fl,em}}$ decreases to a constant value, close to 0.08 V (a value higher than the standard deviations of $\tilde{\phi}_p$). Similar to the first regime, we compare the time series (relative amplitude) of $\tilde{\phi}_{fl,em}(t)$ corresponding to $I_{em} = I^*_{em} = 35$ mA to the plasma potential fluctuations in Fig. 4(b). This time, $\tilde{\phi}_{fl,em}(t|I_{em} = I^*_{em})$ is only slightly phase shifted from $\tilde{\phi}_p(t)$ ($\approx 7°$) but the amplitude difference is now higher than in the first regime (the amplitude of $\tilde{\phi}_{fl,em}(t)$ is now 30% larger than the one of $\tilde{\phi}_p(t)$).

In Fig. 5, the experimental evolution of the standard deviation was also compared to the theoretical one calculated from the first order model using the experimental data

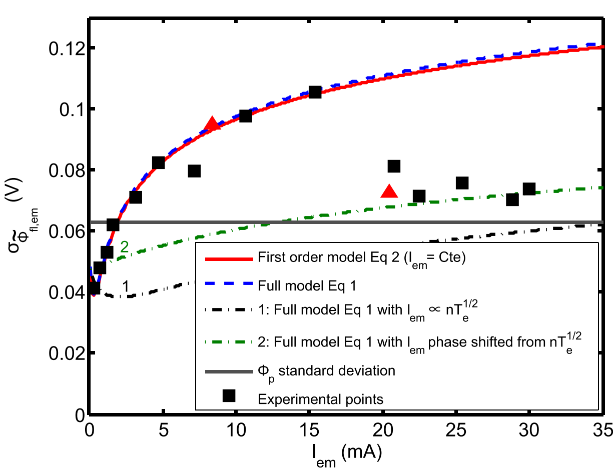

FIG. 5. Standard deviation of the emissive probe floating potential fluctuations $\sigma_{\tilde{\phi}_{fl,em}}$ as a function of the emission current in the regime 2; squares: experimental values, full line: theoretical values calculated using the first order model (Eqs. (2) and (3)), dashed line: theoretical values calculated using the full model (Eq. (1)), 1: black dashed-dotted line: theoretical values calculated using the full model (Eq. (1)) and considering $I_{em} \propto n\sqrt{T_e}$, 2: green dashed-dotted line: theoretical values calculated using the full model (Eq. (1)) and considering the phase-shift experimentally measured between I_{em} and $n\sqrt{T_e}$.

($\tilde{\phi}_p$, $\tilde{n}$, $\tilde{T}_e$, $\langle n\rangle$, $\langle T_e\rangle$, $\langle I_{es}\rangle$, and $\langle I_{is}\rangle$) measured in this second plasma regime (red line). As for the first regime, all the information to calculate the theoretical values from Eq. (1) are available and the corresponding theoretical curve is thus also displayed in Fig. 5 (blue dashed line). Since the plasma modulation levels are still weak, the first order model remains a good approximation and then coincides with the non differentiated relation. In this second regime, the theoretical values are in very good agreement with the experimental points until the emission current reaches $I_{em} = 15$ mA where a discontinuity in the evolution of $\sigma_{\tilde{\phi}_{fl,em}}$ with I_{em} is observed. This model fails in predicting the evolution of the floating potential modulation for $I_{em} > 15$ mA.

IV. EVIDENCE FOR EMISSION CURRENT OSCILLATIONS

The previous theoretical evolutions of $\sigma_{\tilde{\phi}_{fl,em}}$ with I_{em} have been calculated (using either the first order model or the full model) considering two hypothesis: quasi-static sheath and constant emission current. The first hypothesis is valid for all the plasma parameters investigated here. The assumption of a constant emission current is obviously the most fragile in our case. While this assumption is probably fulfilled in the first regime, it seems to break in the second regime above a threshold in emission current corresponding to $I_{em} = 15$ mA. Consequently, it is reasonable to assume that oscillations of the emission current (probably dependent on the plasma parameter fluctuations) are responsible for the discrepancy between the theoretical curves and the experimental points in this second regime.

In order to confirm this hypothesis, two time series of the emission current have been measured in the second plasma regime. One measurement is done for a mean emission current corresponding to $\langle I_{em}\rangle = 8.5$ mA below the threshold of 15 mA and one above, at $\langle I_{em}\rangle = 20$ mA. Time series of the emission current $\tilde{I}_{em}$ have been obtained using the method of time-resolved current-voltage characteristics reconstruction described previously for the heated probe characteristics. A reference set of *I-V* curves corresponding to each time of the periodic modulation are reconstructed using the emissive probe as a cold probe. Sets of *I-V* curves, measured with the heated probe, are reconstructed using the same phase reference (the modulation signal). Instantaneous emitted current characteristics are then defined as the subtraction of the cold characteristic curves from the hot characteristic curves at each time of the modulation. The instantaneous evolution of the emission current is evaluated as the value of this instantaneous emitted current characteristic at the instantaneous floating potential of the heated emissive probe characteristic. The time series for the relative amplitude of $\tilde{I}_{em}(t)$ are shown in Fig. 6 for $\langle I_{em}\rangle = 8.5$ and 20 mA, respectively. To the best of our knowledge, this is the first time that emission current fluctuations are successfully measured. The standard deviations of the floating potential of the emissive probe for these two points are highlighted as two red triangles in Fig. 5.

A significant difference between the fluctuation levels and shapes of $\tilde{I}_{em}$ is observed: the amplitude of $\tilde{I}_{em}$ is almost

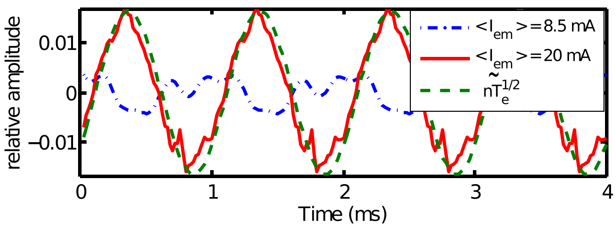

FIG. 6. Relative amplitudes of the emission currents fluctuations corresponding to $\langle I_{em}\rangle = 8.5$ mA and $\langle I_{em}\rangle = 20$ mA as well as the relative amplitude of the fluctuations of the term $n\sqrt{T_e}$.

5 times larger when $\langle I_{em}\rangle = 20$ mA as compared to $\langle I_{em}\rangle = 8.5$ mA. As we show below, this observation explains the discontinuity observed in the standard deviation of the floating potential of the emissive probe at $\langle I_{em}\rangle = 15$ mA. While the assumption of constant emission current holds at low value of $\langle I_{em}\rangle$, it breaks at higher value and modulations of the emission current should be taken into account in Eq. (1) to correctly predict the dependence of the emissive probe floating potential modulation with the plasma parameters modulations.

In addition to this observation, the emission current modulations are compared (Fig. 6) with $n\sqrt{T_e}$ modulations (assuming that saturation currents are proportional to $n\sqrt{T_e}$). The relative amplitude of modulations for I_{em} and $n\sqrt{T_e}$ is similar for $\langle I_{em}\rangle = 20$ mA (same relative amplitude, same frequency). They are however phase shifted by about $\approx 15°$. On the contrary for $\langle I_{em}\rangle = 8.5$ mA, the fluctuations of I_{em} seem more noisy (there are periodic on the plot only because the reconstruction method yields a periodic signal). From these measurements, we have calculated the standard deviation of $\phi_{fl,em}$ as a function of I_{em} according to Eq. (1). Our first calculation assumed an emission current proportional to $n\sqrt{T_e}$ and is shown by the (black) dashed-dotted line in Fig. 5. In this specific case, the calculation differs from the experimental evolution of $\sigma_{\tilde{\phi}_{fl,em}}$ but becomes equal (as expected) to the standard deviation of the plasma potential fluctuations when $I_{em} = I^*_{em} = 35$ mA. A second calculation has been carried out considering the phase-shift and the amplitude of $\tilde{I}_{em}$ experimentally measured at $\langle I_{em}\rangle = 20$ mA and assuming that the relative oscillation of I_{em} remains constant in the range of $\langle I_{em}\rangle \in [0-35]$ mA. The corresponding theoretical evolution is shown in Fig. 5 as a (green) dashed-dotted line. One can now notice that the theoretical values are in good agreement with the experimental points in the range $\langle I_{em}\rangle \in [20-35]$ mA for which it is clear that the fluctuations of the emission current are not negligible.

We now discuss physical processes which would lead to emission current modulations. We recall here that the main purpose of this article is to check the validity of Eq. (2) for the interpretation of emissive probe measurements. This section shows that fluctuations of I_{em} should also be taken into account. Formally, this means that a term $(\langle T_e\rangle/\langle I_{is}+I_{em}\rangle)\tilde{I}_{em}$ should be added to Eq. (2).

A precise determination of the physical process leading to fluctuations of I_{em} is beyond the scope of the present article and is likely to strongly depend on details of the time-averaged plasma parameters and their fluctuations dynamics. The following discussion thus raises questions that should be addressed in the near future for understanding fluctuations of I_{em}, i.e., expressing these fluctuations as function of the time-averaged plasma parameters and their fluctuations $\tilde{\phi}_p$, $\tilde{n}$, and $\tilde{T}_e$.

Let us first consider a space charge limited current regime (associated to the appearance of a virtual cathode, i.e., an electric potential minimum detached from the probe) as predicted by Hobbs and Wesson.[21] This hypothesis is likely not correct in our case. Indeed, the emission current can still be increased from 15 mA to 35 mA (so that the mean floating potential of the emissive probe eventually reaches the mean plasma potential), whereas in a pure space charge limited regime, current emission should saturate and remains constant when the heating current is increased. According to the literature,[13,22,23] this might be due to the fact that the plasma studied is cold so that the temperature of emitted electrons is small but not negligible compared to the temperature of plasma electrons. In that case, the appearance of a virtual cathode makes the emitted current different from the Richardson current (and dependent on plasma parameters) but does not limit it.

Another phenomenon that should be examined is electron secondary emission. For an incident electron current I_e, the secondary emission current is $\gamma\, I_e$, with γ the electron secondary emission coefficient. The fraction of the emitted current due to this phenomenon oscillates like I_e. For Tungsten and incident electron energy between 1 and 10 eV, γ is between one tenth and four tenth and is very sensitive to incident electron energy.[24,25] Then, as soon as ion current is negligible compared to electron current and if all electrons from the plasma incident on the probe actually hit its surface, the relative amplitude of emission current fluctuations should be between one and four tenth of the relative amplitude of electron current fluctuations which is not enough to explain our observations: in regime 2, both are found to have the same amplitude. However, we should be careful about the definition given of the emitted current I_{em} in this article: it is the difference between the cold probe *I-V* characteristic and the hot probe characteristic at the floating potential of the hot probe. This difference can be due to an electron flux emitted from the surface of the probe or to a diminution of incident electron flux from the plasma on the probe, for example, due to a virtual cathode that reflects a part of incident electrons. This would yield a higher effective secondary emission coefficient, closer to one. According to Hobbs and Wesson the potential barrier is found to be as high as about $T_e/2$; when a non vanishing temperature is considered for electrons emitted from the probe this high could be changed.

V. CONCLUSION

In this paper, we have presented a set of two experiments for which the RF power generating the plasma has been modulated to produce stationary plasma density, plasma potential, and electron temperature fluctuations. Using the time-resolved current-voltage characteristic reconstruction method, we have been able to measure different *I-V* characteristics corresponding to each time of the modulation signal. Synchronization of these measurements with the modulated power has allowed to reliably measure the fluctuations of the three main plasma parameters (n, T_e, and ϕ_p) both in amplitude and phase. Thanks to this experimental arrangement, we have compared the floating potential fluctuations of an emissive probe with the ones of the plasma potential in two regimes.

In the first regime case, the variation of the standard deviation of emissive probe potential with the emission current is in good agreement with the variation predicted by the quasi-static model assuming a constant emission current. However, this is a particular regime as the standard deviation of the fluctuations of $\phi_{fl,em}(t)$ approaches circumstantially the one of $\phi_p(t)$. Indeed, the discrepancy is weak: only 15%, but there is a significant phase shift of 35° between $\phi_{fl,em}(t)$ and $\phi_p(t)$. It is worth reminding that both the amplitude and the phase of the electric field and thus of the plasma potential should be measured precisely for cross-field transport estimation. Such an error on the phase between density and potential fluctuations can result into changing the sign of the turbulent plasma flux in case of drift wave turbulence.

In the second regime case, the model predicts differences between the standard deviation of the emissive probe potential and the standard deviation of the plasma potential when $I_{em} = I^*_{em} = 35\,\mathrm{mA}$ (i.e., when the mean floating potential of the emissive probe is equal to the mean plasma potential). It is not the case as experimental points go off the model curve from $I_{em} = 15\,\mathrm{mA}$. Eventually, the floating potential oscillations at I^*_{em} are in that case almost in phase with plasma potential oscillation but their standard deviation is 30% higher. The reconstructed emission current time series is found to oscillate almost as $n\sqrt{T_e}$ for $I_{em} > 15\,\mathrm{mA}$, whereas it does not significantly vary for $I_{em} < 15\,\mathrm{mA}$. The emission current is found to be phase shifted with respect to $n\sqrt{T_e}$ and the phase shift is found to influence the standard deviation of the floating potential of the emissive probe as expected from Eq. (1). Taking into account both the amplitude and phase of the emission current fluctuations have allowed to recover experimental observations.

In this article, extended experimental validation of the model proposed previously in Ref. 12 has been applied to cases with controlled low-frequency oscillations of $\tilde{n}$ and $\tilde{T}_e$. We showed that this model adequately describes the relationship between $\tilde{\phi}_{fl,em}$, $\tilde{\phi}_p$, $\tilde{n}$, and $\tilde{T}_e$ when the assumption of constant emission current holds. When this assumption fails, an adequate description of the emission current oscillation is required. Moreover, we only considered the case of small relative oscillation amplitude. High relative oscillation amplitude would most probably add non-linearity that might complicate the relations between those variables.

This shows that more experimental and theoretical efforts are needed to identify the plasma parameter domain in which floating potential fluctuation of an emissive probe at $I_{em} = I^*_{em}$ can yield reliable measurement of plasma potential fluctuations. Therefore, the conditions for emission current oscillations to appear and their relationship in phase and amplitude with density and temperature fluctuations have to be elucidated.

ACKNOWLEDGMENTS

This work has been funded by the French National Research Agency through contract Jeune Chercheuse/Jeune Chercheur ANR-13-JS04-0003-01. We acknowledge support by the LABEX iMUST (ANR-10-LABX-0064) of Université de Lyon, within the program "Investissements d'Avenir" (ANR-11-IDEX-0007) operated by the French National Research Agency. This work was also supported by the French National Research Agency through contract ANR-11-BS09-023-03 Sediba.

[1]J. Sheehan and N. Hershkowitz, Plasma Sources Sci. Technol. **20**, 063001 (2011).
[2]N. Mahdizadeh, F. Greiner, M. Ramisch, U. Stroth, W. Guttenfelder, C. Lechte, and K. Rahbarnia, Plasma Phys. Controlled Fusion **47**, 569 (2005).
[3]R. Schrittwieser, C. Ionita, P. Balan, R. Gstrein, O. Grulke, T. Windisch, C. Brandt, T. Klinger, R. Madani, G. Amarandei, and A. K. Sarma, Rev. Sci. Instrum. **79**, 083508 (2008).
[4]R. Schrittwieser, C. Ionita, P. Balan, C. Silva, H. Figueiredo, C. Varandas, J. Juul Rasmussen, and V. Naulin, Plasma Phys. Controlled Fusion **50**, 055004 (2008).
[5]R. Schrittwieser, J. Adamek, P. Balan, M. Hron, C. Ionita, K. Jakubka, L. Kryska, E. Martines, J. Stöckel, M. Tichy, and G. Van Oost, Plasma Phys. Controlled Fusion **44**, 567 (2002).
[6]J. Adamek, J. Horacek, J. Seidl, H. Müller, R. Schrittwieser, F. Mehlmann, P. Vondracek, S. Ptak, C. Team, and A. U. Team, Contrib. Plasma Phys. **54**, 279 (2014).
[7]P. Balan, R. Schrittwieser, C. Ionita, J. A. Cabral, H. Figueiredo, H. Fernandes, C. Varandas, J. Adamek, M. Hron, J. Stöckel, E. Martines, M. Tichy, and G. Van Oost, Rev. Sci. Instrum. **74**, 1583 (2003).
[8]C. Ionita, P. Balan, R. Schrittwieser, H. Figueiredo, C. Silva, C. Varandas, and R. Galvao, Rev. Sci. Instrum. **75**, 4331 (2004).
[9]G. Bousselin, Ph.D. thesis, Université de Lorraine, 2013.
[10]G. Bousselin, J. Cavalier, J. F. Pautex, S. Heuraux, N. Lemoine, and G. Bonhomme, Rev. Sci. Instrum. **84**, 013505 (2013).
[11]C. Ionita, J. Grünwald, C. Maszl, R. Stärz, M. Cercek, B. Fonda, T. Gyergyek, G. Filipic, J. Kovacic, C. Silva, H. Figueiredo, T. Windisch, O. Grulke, T. Klinger, and R. Schrittwieser, Contrib. Plasma Phys. **51**, 264 (2011).
[12]G. Bousselin, N. Lemoine, J. Cavalier, S. Heuraux, and G. Bonhomme, Rev. Sci. Instrum. **85**, 056102 (2014).
[13]S. Takamura, N. Ohno, M. Ye, and T. Kuwabara, Contrib. Plasma Phys. **44**, 126 (2004).
[14]M. Ye and S. Takamura, Phys. Plasmas **7**, 3457 (2000).
[15]N. Plihon, G. Bousselin, F. Palermo, J. Morales, W. J. T. Bos, J. Godeferd, M. Bourgoin, J. F. Pinton, M. Moulin, and A. Aanesland, J. Plasma Phys. **81**, 345810102 (2015).
[16]I. D. Sudit and F. F. Chen, Plasma Sources Sci. Technol. **3**, 162 (1994).
[17]N. Plihon, C. Corr, P. Chabert, and J. Raimbault, J. Appl. Phys. **98**, 023306 (2005).
[18]More precisely, the emitted current depend both on the heating current I_h and on the value of the probe voltage bias V. The emitted current is defined by subtracting the cold probe I-V characteristic $I(V|I_h = 0A)$ from the heated probe characteristic $I(V|I_h)$ and the emission current is the value of the emitted current at the floating potential of the heated characteristic.
[19]P. Chabert and N. Braithwaite, *Physics of Radio-Frequency Plasmas* (Cambridge University Press, 2011).
[20]C. Ionita, P. Balan, T. Windisch, C. Brandt, O. Grulke, T. Klinger, and R. Schrittwieser, Contrib. Plasma Phys. **48**, 453 (2008).
[21]G. D. Hobbs and J. A. Wesson, Plasma Phys. **9**, 85 (1967).
[22]G. D. Porter, Nucl. Fusion **22**, 1279–1289 (1982).
[23]T. Gyergyek and J. Kovacic, Contrib. Plasma Phys. **52**, 699 (2012).
[24]E. W. Thomas, Nucl. Fusion Suppl. **1**, 79–91 (1991).
[25]I. H. Khan, J. P. Hobson, and R. A. Armstrong, Phys. Rev. **129**, 1513 (1963).